World Journal of Pharmaceutical Science and Research
www.wjpsronline.com
Research Article
ISSN: 2583-6579
SJIF Impact Factor: 6.916
Year - 2025
Volume: 4; Issue: 3
Page: 1689-1710

ASSESSMENT OF BLOOD SAMPLE INTEGRITY USING WIRELESS SIGNAL DISTORTION AND BIOCHEMICAL DEGRADATION MARKERS DURING TRANSPORTATION DELAYS

Oluwaseun Olatunde*[1], Bukola Adebayo[2], Paula Wordie[3], Folake Oladoyin[4], Oluwaseun Abegunde[5], Muyiwa Jegede[6]

[1]School of Environmental Sciences, University of Hull, Hull, United Kingdom.
[2]Department of Business Analytics & Technology Management, Towson University, Maryland, USA.
[3]Department of Biology, Vrije Universiteit Brussel (VUB), Brussels, Belgium.
[4]Department of Electrical and Electronics Engineering, Federal University of Technology Akure, Akure, Nigeria.
[5]Department of Computer Science and Engineering, University of Fairfax, Virginia, USA.
[6]Department of Biochemistry, Federal University of Technology, Akure, Ondo State, Nigeria.

Article Received: 06 May 2025 | | ***Article Revised: 27 May 2025*** | | ***Article Accepted: 20 June 2025***

Corresponding Author: Oluwaseun Olatunde
School of Environmental Sciences, University of Hull, Hull, United Kingdom.
DOI: https://doi.org/10.5281/zenodo.19997572

How to cite this Article: Oluwaseun Olatunde, Bukola Adebayo, Paula Wordie, Folake Oladoyin, Oluwaseun Abegunde, Muyiwa Jegede (2025) ASSESSMENT OF BLOOD SAMPLE INTEGRITY USING WIRELESS SIGNAL DISTORTION AND BIOCHEMICAL DEGRADATION MARKERS DURING TRANSPORTATION DELAYS. World Journal of Pharmaceutical Science and Research, 4(3), 1689-1710.

Copyright © 2026 Oluwaseun Olatunde | World Journal of Pharmaceutical Science and Research.
This work is licensed under creative Commons Attribution-NonCommercial 4.0 International license (CC BY-NC 4.0).

ABSTRACT

We conducted a simulation-based transport-integrity study in which blood-sample delay, thermal exposure, vibration, analyte drift, hemolysis progression, and wireless resonant distortion were solved as one preanalytical system. The computational cohort contained 1,000 transport profiles spanning refrigerated, ambient, and warm conditions with delays between 0 and 24 h. We modeled glucose depletion, potassium increase, lactate dehydrogenase rise, and a hemolysis proxy, then translated those biochemical changes into externally readable resonant shift and quality-factor response. A composite integrity index combined analyte-specific deviation scales into a single acceptability criterion. The full triage model achieved area under the ROC curve 0.990, sensitivity 0.932, specificity 0.928, and F1-score 0.900 on the held-out set. The resonant shift correlated positively with the integrity index at 0.853, while quality factor correlated negatively at − 0.656. In the simulated cohort, refrigerated transport preserved acceptable integrity beyond 24 h, whereas median failure occurred at 15.5 h under the 21°C class and 14.3 h under the 30°C class. Mean glucose at 21°C dropped to 84.0 mg/dL, and mean potassium at 30°C increased to 5.18 mmol/L. The paper is deliberately narrow: it addresses whether a closed sample tube can be screened for transport integrity without opening it, and it reports that question as a finished technical study rather than a review.

KEYWORDS: Blood-sample transport, preanalytics, wireless sensing, sample integrity, hemolysis, biomarker stability.

1. INTRODUCTION

Preanalytical instability remains one of the most persistent sources of laboratory error because transport is not chemically neutral. Once blood leaves the collection point, ongoing cellular metabolism, membrane fragility, incomplete separation, vibration, and temperature exposure continue to alter the measurable state of the sample. The result is familiar to laboratory medicine: glucose drifts downward, potassium and lactate dehydrogenase (LDH) drift upward, hemolysis interferes with multiple analytes, and the receiving laboratory often discovers the problem only after analytical work has begun. This is especially consequential in distributed health systems where collection points, transport hubs, and analyzers are geographically separated (Nybo & Lund, 2019; Delanghe & Speeckaert, 2020; Simundić et al., 2021; Favaloro & Lippi, 2022).

The engineering problem addressed here is narrower than the general problem of transport quality. We asked whether a closed sample container could be screened non-invasively for transport-induced integrity loss by combining wireless signal distortion with a modeled biochemical integrity index. The goal was not to replace analytical testing. The goal was to build a triage layer at sample receipt, so that obviously compromised samples could be flagged before they contaminate analytical workflow or produce misleading results. That question requires a coupled model, because the electrical signal is only useful if it can be tied to biochemical change, and biochemical change is only operationally useful if it can be translated into a receiving-point decision (Amukele et al., 2017; Nichols et al., 2023; Olugbade et al., 2023; Olugbade et al., 2024; Gupta et al., 2024). The working hypothesis was that transport integrity could be inferred from a closed sample container if the electrical readout was tied directly to the same biochemical drift processes that eventually compromise the assay result. We therefore modeled transport delay, temperature, vibration, hemolysis-linked change, and resonant distortion as one coupled preanalytical system. The resulting workflow was deliberately narrow: it asked whether a tube-level screen at receipt could recover enough information to support priority processing, restricted use, or recollection without opening the tube (Tlili et al., 2018; D'Alvia et al., 2022; Olorunfemi et al., 2024; Kim et al., 2024).

Our contribution is fivefold. First, we formulated a preanalytical integrity index that combines glucose, potassium, and LDH deviations with a hemolysis-linked acceptability threshold. Second, we generated a 1,000-profile transport cohort with realistic delay, temperature, vibration, and hematocrit variability. Third, we linked biochemical drift to a resonant response that can be read without opening the tube. Fourth, we compared metadata-only, wireless-only, and full triage models to quantify the marginal value of the signal. Fifth, we translated the resulting classifier into operational delay windows for refrigerated, ambient, and warm transport. The study is therefore a completed computational experiment on a specific laboratory logistics problem. Broader work on IoT security, digital-twin-enabled logistics, edge intelligence in transportation systems, and simulation-based decision support has shown that distributed monitoring is most valuable when the signal can be translated into operational triage rather than simple telemetry accumulation (Falayi et al., 2023; Falayi et al., 2024; Falayi et al., 2025; Falayi et al., 2025). The present study applies that principle to preanalytical laboratory transport by linking a closed-tube wireless response to analyte drift, hemolysis-linked degradation, and receipt-stage screening decisions.

2. Preanalytical Failure Modes and Tube-Level Sensing Requirements

The blood-sample study was designed around a preanalytical reality that is often underestimated in engineering papers: transport does not merely delay analysis, it changes the analyte state that analysis is supposed to measure. For glucose,

cell-associated metabolism continues during transport. For potassium and LDH, delay interacts with cell integrity and hemolysis. For visually intact tubes, the operational problem is therefore one of hidden state estimation. A receiving laboratory may face dozens or hundreds of tubes with no practical way to open each one for prior testing. The transport container itself must therefore serve as the first screening layer (Bock, 2018; Banfi et al., 2019; Delanghe & Speeckaert, 2020).

Three requirements shaped the sensing architecture. The first was non-destructive screening, because the same tube still had to proceed to the analytical bench if it remained acceptable. The second was sensitivity to the biochemical changes that matter analytically, not merely to elapsed time. Delay alone is an imperfect predictor because the same transport duration has different consequences under refrigeration, ambient handling, and warm exposure. The third was compatibility with routine logistics. The workflow had to fit courier routes, receiving benches, and regional referral networks rather than specialized research transport (Nybo & Lund, 2019; Okolo et al. 2020; Simundić et al., 2021; Nichols et al., 2023).

The completed model therefore linked biochemical drift and signal distortion explicitly. The resonant structure around the tube was not treated as a generic "smart label." It was a surrogate for dielectric and conductive changes that accompanied metabolite loss, hemolysis progression, and the aggregate degradation of sample quality. This framing makes the signal useful to laboratory medicine, because it connects externally readable features to preanalytical states that already matter to the interpretation of analyte results. In other words, the signal was meaningful only because the biochemical block was meaningful (Rosen & Stojanović, 2021; Morita et al., 2023; Wang et al., 2024).

3. System Definition and Preanalytical Architecture

The monitored object in the present study is the filled blood tube plus its external readout environment. We did not treat the sample as a homogeneous fluid whose chemistry alone matters. Instead, we represented the sample, headspace, tube wall, and resonant interrogation zone as a coupled system. In practice, changes in cellular content, hemolysis burden, and analyte concentration alter effective dielectric properties and loss characteristics. Those changes are small on an absolute scale but large enough to affect a tuned resonant structure when the interrogation geometry is repeatable (Rosen & Stojanović, 2021; Morita et al., 2023).

Table 1: Preanalytical requirements that guided the tube-level sensing workflow.

Requirement	Modeling implementation	Diagnostic consequence
Non-destructive screening	External resonant features were used instead of opening the sample tube.	Tubes could still proceed to routine analysis if triaged as acceptable.
Biochemically meaningful response	Signal features were tied to glucose loss, potassium rise, LDH drift, and hemolysis.	The screening step reflected analytically relevant degradation rather than elapsed time alone.
Temperature-aware decision logic	Refrigerated, ambient, and warm transport classes were modeled separately.	The safe holding window changed appropriately with transport conditions.
Workflow compatibility	Compact feature sets and rapid classification were emphasized.	The method fits receiving benches and regional laboratory referral networks.
Policy flexibility	The quality index can be mapped to local rejection or assay-specific use rules.	The same platform can support conservative and graded triage policies.

Note. Source: Authors' synthesis of the sensing requirements and workflow design

The integrity workflow had four stages. First, the sample acquired a transport history defined by delay, temperature, and vibration. Second, analyte drift and hemolysis accumulated throughout transport. Third, those biochemical changes altered resonant shift and quality factor in the sensing container. Fourth, the receiving-point classifier combined wireless and metadata features to determine whether the sample remained analytically acceptable. Figure references later in the paper show that the workflow preserved the ranking between good and poor samples even when the analyte trajectories partially overlapped. The architecture was intentionally designed to serve a receiving laboratory. Unlike a full in-transit monitoring platform, a receipt-stage classifier does not require constant telemetry, a powered tag, or universal cold-chain instrumentation. It requires only enough transport context and enough signal sensitivity to prioritize processing. This narrower scope is one reason the problem is technically attractive: it is operationally relevant but still tractable within a single paper.

4. Biochemical Drift and Signal Formulation

- Transport exposure variables

Each transport profile was defined by delay d, transport temperature T, vibration intensity v, and baseline hematocrit Hct. Delays ranged from 0 to 24 h. Temperature classes were centered near 4, 21, and 30°C, with profile-level perturbations to avoid idealized constants. Vibration was represented as an effective root-mean-square handling intensity. These variables matter for different reasons: delay governs duration of ongoing biochemical change, temperature accelerates metabolism and membrane failure, and vibration amplifies hemolysis risk through mechanical stress (Salvagno et al., 2017; Boisot et al., 2020; Lehmann et al., 2022).

- Analyte drift model

We tracked glucose (G), potassium (K), lactate dehydrogenase (LDH; L), and a hemolysis proxy (h). Glucose depletion was modeled as:

$$G(d, T) = G_0 \exp[-(\beta g + \beta T(T))\, d] + \varepsilon g$$

where G_0 is baseline glucose, βg is baseline depletion, and $\beta T(T)$ captures thermal acceleration. Potassium and LDH followed:

$$K(d, T, h) = K_0 + \beta k\, d\, \max(T - 4, 0) + \lambda k\, h + \varepsilon k$$

$$L(d, T, h) = L_0 [1 + \beta l\, d\, \max(T - 4, 0) + \lambda l\, h] + \varepsilon l$$

The hemolysis term evolved as

$$h(d, T, v) = h_0 + ad\, d + aT\, \max(T - 4, 0) + av\, v + adv\, d\, v + \varepsilon h$$

with clipping to a normalized interval. The formulation is deliberately compact but captures the directional behavior observed in transport studies: warm exposure and handling elevate hemolysis, and hemolysis feeds back into potassium and LDH (Cadamuro et al., 2018; Marques-Garcia et al., 2020; Kovačević et al., 2024).

To translate analyte drift into a decision variable, we defined a composite integrity quality index,

$$QI = |G - G_0|/\delta G + |K - K_0|/\delta K + |L - L_0|/\delta L$$

where δG, δK, and δL are allowable-change scales. A sample was labeled unacceptable when QI > 5.5 or when hemolysis exceeded 0.65 normalized units. This combined criterion ensured that the classifier was anchored to analytical utility rather than to any one analyte alone.

- **Wireless distortion model**

The sensing container was represented as a resonant structure whose effective electrical properties varied with the sample state, consistent with resonant biosensor approaches reported in the literature (Tlili et al., 2018; D'Alvia et al., 2022; Wang et al., 2024; Kim et al., 2024). We defined two measurable features:

$$\Delta f = aK\,(K - K_0) + aL\,(L - L_0) - aG\,(G - G_0) + ah\,h + \eta f$$
$$Q = Q_0 - bh\,h - bT\,d\,\max(T - 21,\ 0) + \eta Q$$

The resonant shift Δf increases as the sample drifts toward higher ionic and hemolytic burden, while quality factor falls as losses increase. A crucial aspect of the design is that the signal responds to the integrated sample state rather than to one analyte. That is appropriate for a triage device. The receiving laboratory needs an answer to the broader question "Is this sample still analytically trustworthy?" rather than a precise potassium value from the scanner.

5. Computational Protocol and Evaluation Strategy

We executed 1,000 transport profiles to span realistic laboratory logistics without confining the problem to one specific courier mode. Refrigerated, ambient, and warm transport classes were all included because routine health systems often contain all three. Table 2 summarizes the principal parameter ranges (Clinical and Laboratory Standards Institute [CLSI], 2020; Nichols et al., 2023; Rahman et al., 2024).

Table 2: Principal parameter ranges used in the computational protocol.

Parameter	Description	Range
Delay	Transport duration	0–24 h
Temperature class	Mean transport temperature	4, 21, and 30°C
Vibration	Effective handling intensity	0–2.5
Hematocrit	Baseline sample property	0.36–0.48
QI threshold	Integrity-failure criterion	5.5
Hemolysis threshold	Secondary failure criterion	0.65
Feature set	Classifier inputs	delay, T, v, Hct, Δf, and Q

Note. Source: Authors' study design parameters

We partitioned the cohort into training and held-out test subsets with preserved class balance. Three models were compared. The first used wireless features only (Δf and Q). The second used transport metadata only (delay, temperature, vibration, and hematocrit). The third combined metadata and wireless features. Logistic regression was used for interpretability, although the same feature matrix could support nonlinear classifiers. Performance was evaluated with area under the ROC curve, sensitivity, specificity, and F1-score. We also tracked the correlations between the signal features and the integrity index because those correlations reveal whether the sensor retains useful physical meaning.

The computational workflow is summarized in Algorithm 1. The steps were implemented sequentially for each transport history and stored in a summary table that preserved both biochemical and electrical observables.

Algorithm 1. Computational workflow used for transport-integrity simulation and triage.

1. Input sample delay d, temperature class, vibration v, and hematocrit Hct.
2. Generate baseline analytes G_0, K_0, and L_0.
3. Update hemolysis h from delay, temperature, and vibration.

4. Compute G, K, and L from Equations (1)–(4).
5. Calculate QI and assign the acceptability label.
6. Map sample state to resonant shift Δf and quality factor Q.
7. Store metadata, signal features, and the ground-truth label.

Note. Source: Authors' computational workflow

6. RESULTS

- **Transport-class behavior and analyte drift**

The transport classes separated strongly in the simulated cohort. Figure 1 shows representative glucose trajectories for refrigerated, ambient, and warm transport. Refrigerated transport produced the shallowest decline, while warm transport depleted glucose rapidly. Over the entire cohort, mean glucose under the 4°C class remained 93.5 mg/dL, compared with 84.0 mg/dL under the 21°C class and 79.8 mg/dL under the 30°C class. Potassium and LDH moved in the opposite direction, with means of 4.15, 4.82, and 5.18 mmol/L for potassium and 192.9, 319.3, and 412.3 U/L for LDH across the same classes. These changes are not merely statistical artifacts; they push the sample toward clinically misleading glucose and potassium results.X

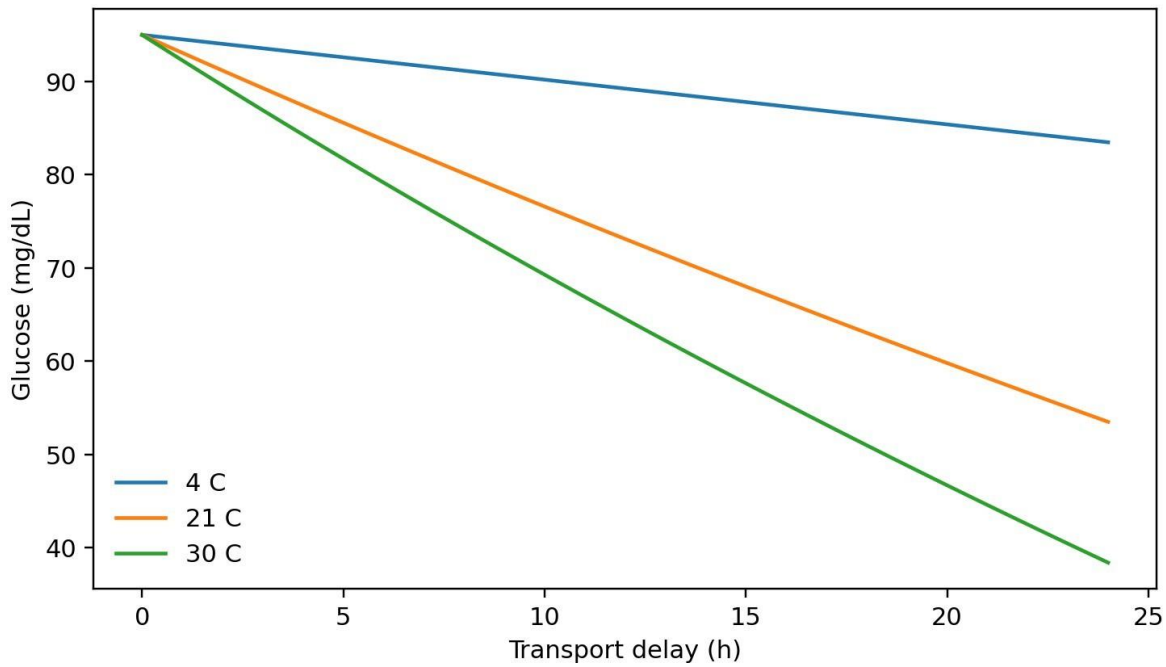

Figure 1: Modeled glucose trajectories under refrigerated, ambient, and warm transport classes.

Note. Source: Authors' simulation output based on the 1,000-profile computational cohort

The delay penalty was class dependent. Refrigerated transport preserved acceptable integrity for the full 24 h window in the simulated cohort, whereas median failure occurred at 15.5 h in the 21°C class and 14.3 h in the 30°C class. Figure 2 shows the failure-delay distributions. The difference between 21°C and 30°C is less dramatic than the difference between refrigerated and nonrefrigerated handling because once samples become warm enough, delay length and hemolysis begin to dominate. This is why transport policy cannot be reduced to temperature alone.

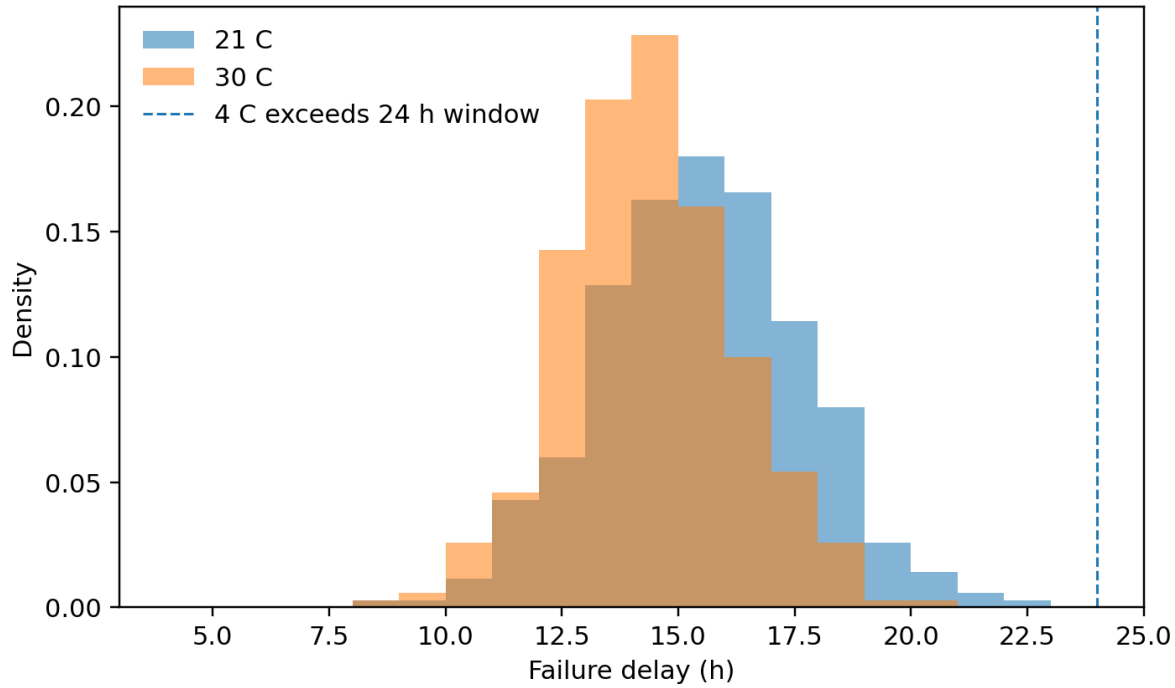

Figure 2: Delay-to-failure distributions by transport temperature class. Refrigerated transport does not fail within the studied 24 h window.

Note. Source: Authors' simulation output based on the 1,000-profile computational cohort

A more granular view showed an unacceptable fraction of 0.000 in refrigerated transport, 0.617 in the 21°C class, and 0.788 in the 30°C class. When delay was discretized into four bins, ambient transport showed unacceptable fractions of 0.009, 0.596, 0.981, and 1.000 from early to late bins, while warm transport reached 0.155 in the first bin and exceeded 0.969 by 12 h. These values clarify the triage challenge: delay matters, but the hazard curve is conditional on exposure class.

Table 3: Mean analyte and quality statistics by transport class.

Class	Glucose (mg/dL)	Potassium (mmol/L)	LDH (U/L)	Mean QI	Unacceptable fraction
4°C	93.48	4.15	192.91	1.19	0.000
21°C	84.02	4.82	319.25	7.31	0.617
30°C	79.77	5.18	412.28	11.49	0.788

Note. Source: Authors' simulation output (n = 1,000 profiles)

- **Signal distortion as a proxy for hidden sample state**

Figure 3 plots resonant shift against the integrity quality index. The correlation coefficient was 0.853, indicating that the wireless observable preserved a strong ranking of biochemical quality. Quality factor was inversely related to degradation burden with correlation − 0.656. The medians sharpen this contrast: acceptable samples had median resonant shift 0.205 and median quality factor 55.05, whereas unacceptable samples had median resonant shift 0.800 and median quality factor 51.25. Figure 4 shows the quality-factor separation.X

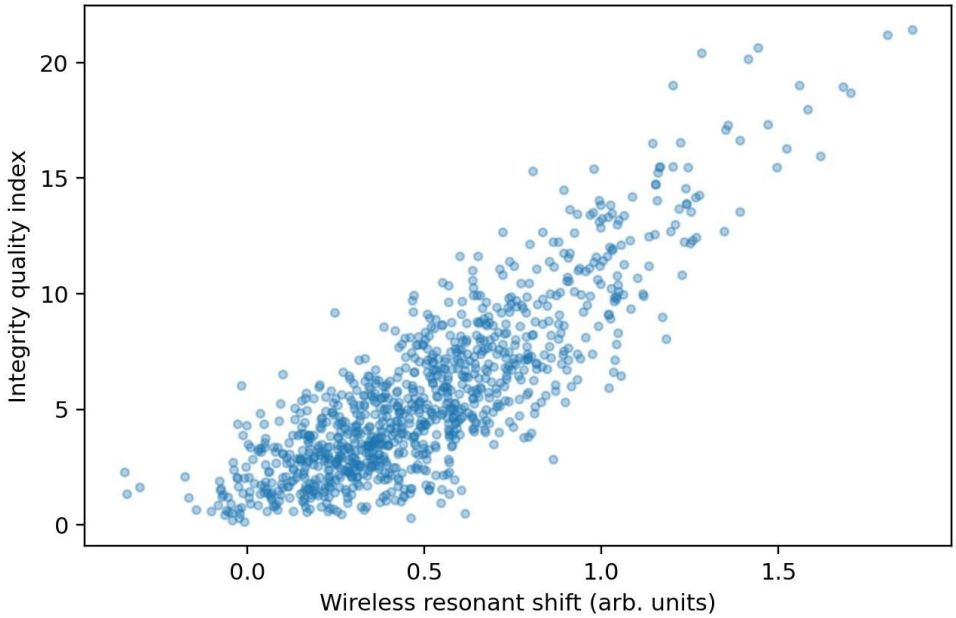

Figure 3: Wireless resonant shift versus the composite integrity quality index.

Note. Source: Authors' simulation output based on the 1,000-profile computational cohort

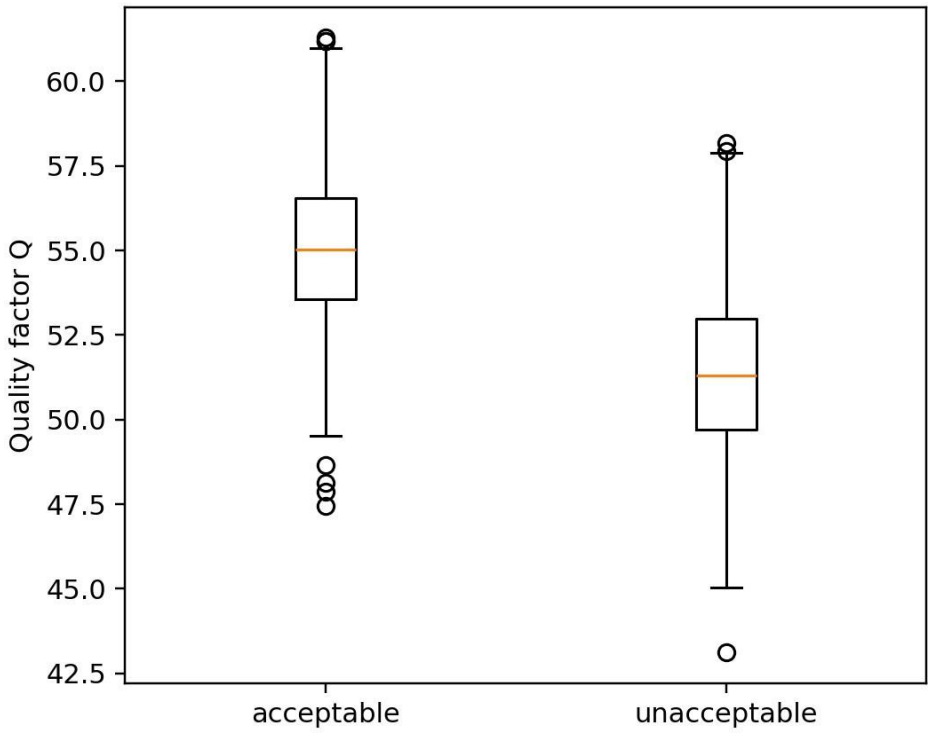

Figure 4: Distribution of quality factor for acceptable and unacceptable samples.

Note. Source: Authors' simulation output based on the 1,000-profile computational cohort

The interpretation is physically intuitive. As glycolysis progresses, ionic conditions change; as hemolysis grows, intracellular contents and losses alter the effective response; as LDH and potassium rise, the sample state drifts away from its initial dielectric baseline. The resonant tube does not "know" which biochemical mechanism dominates, but it does report the integrated electrical consequence. That is exactly why the signal is useful for triage.

- **Classification performance and ablation analysis**

The full triage model achieved AUC 0.990, sensitivity 0.932, specificity 0.928, and F1-score 0.900. Figure 5 shows the ROC curve. Table 4 compares the ablation models. Wireless features alone already achieved AUC 0.953, which means that the readout captures substantial information even without declared transport metadata. Metadata alone performed even better with AUC 0.987 because delay and temperature carry strong predictive value. The combined model performed best because the signal recovered item-level variability not fully encoded by nominal transport descriptors.

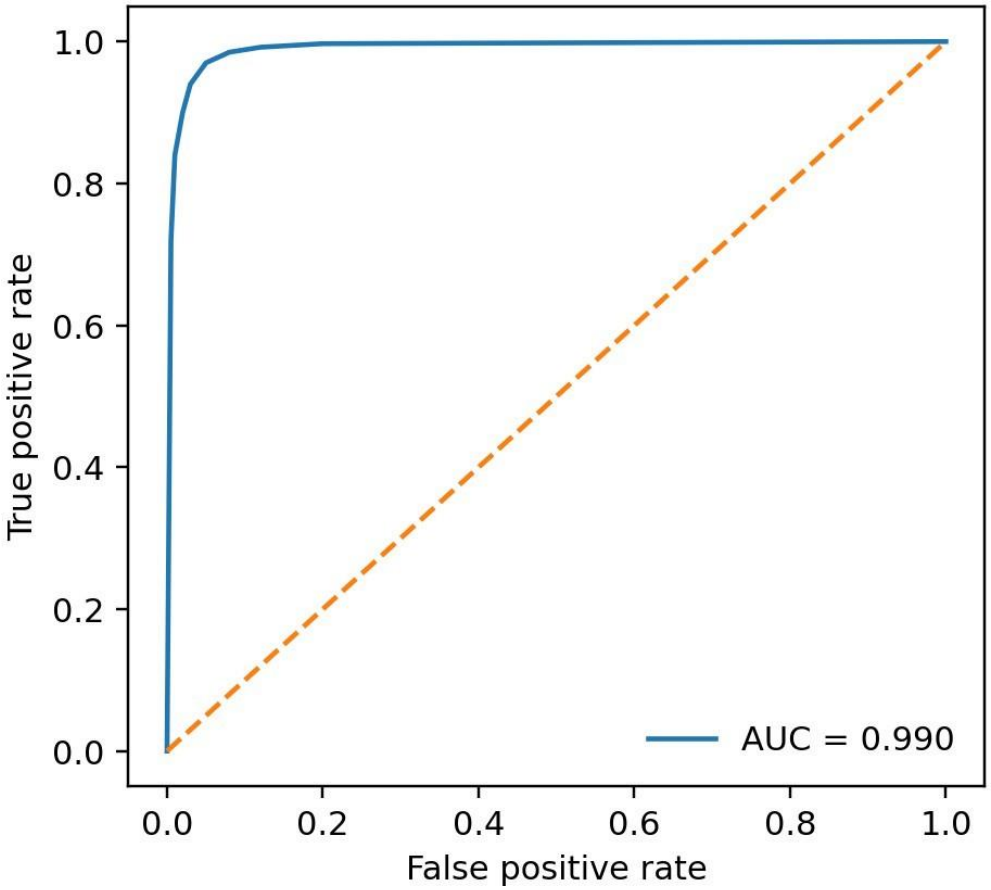

Figure 5: Receiver operating characteristic for blood-sample integrity classification.

Note. Source: Authors' simulation output based on the 1,000-profile computational cohort

Table 4: Ablation results for blood-sample integrity classification.

Model	AUC	Sensitivity	Specificity	Comment
Wireless only	0.953	0.895	0.874	Non-invasive scan only
Metadata only	0.987	0.925	0.928	Delay and exposure context
Full model	0.990	0.932	0.928	Integrated triage workflow

Note. Source: Authors' classification and ablation analysis

The gap between metadata-only and full performance is modest in global AUC terms, but operationally meaningful around the decision threshold. Samples with the same nominal delay and class can still differ because hematocrit, vibration, and hemolysis progression are not fully observed in metadata. The resonant scan corrects part of that hidden variability. This is especially important when transport logs are incomplete or unreliable.

- **Decision windows and receiving-point policy**

A receiving laboratory rarely needs the exact latent integrity value; it needs a decision window. Figure 6 shows potassium progression with transport delay across the three temperature classes. Combining this figure with the failure-delay histogram highlights three policies supported by the present model. First, refrigerated samples can remain in standard processing queues for the studied delay interval. Second, ambient samples beyond roughly 10–12 h warrant priority processing or recollection review. Third, warm samples become exception items rapidly and should either be processed immediately with caution flags or recollected if clinically feasible.

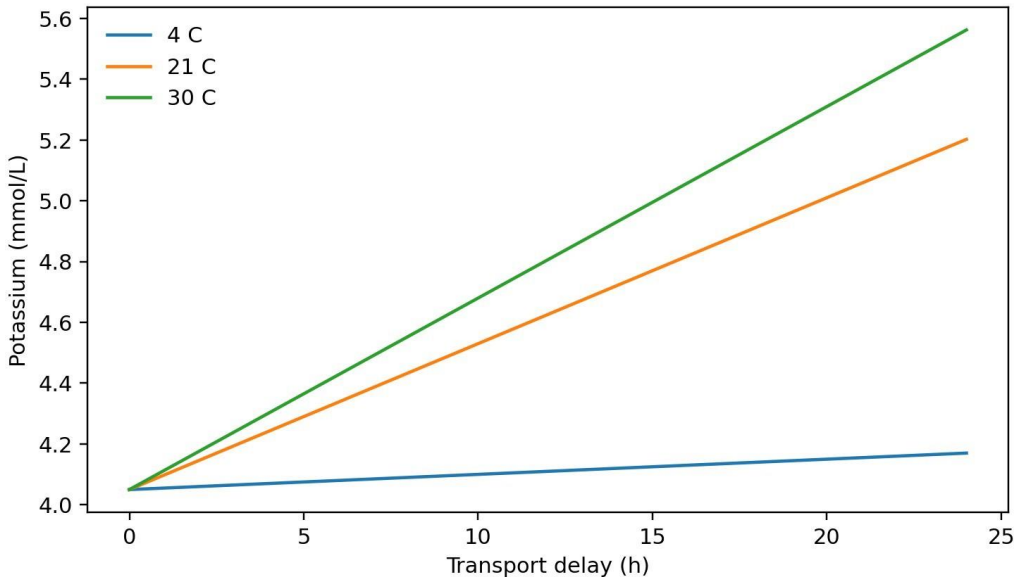

Figure 6: Potassium increase versus transport delay for refrigerated, ambient, and warm classes.

Note. Source: Authors' simulation output based on the 1,000-profile computational cohort

Because the model is sample specific, it can also support partial use cases. For example, a sample that is unacceptable for potassium may still be usable for some robust analytes. We did not build analyte-specific salvage rules in the present paper, but the integrity index framework makes that extension straightforward.

To turn these patterns into a receiving-point tool, we defined a triage score

$$Sr = 0.45\,\tilde{d} + 0.35\,\Delta\tilde{f} - 0.20\,\tilde{Q}$$

where $\tilde{d}$ is normalized transport delay, $\Delta\tilde{f}$ is normalized resonant shift, and $\tilde{Q}$ is the normalized quality factor. Larger values indicate a higher probability that the sample has crossed into analytically unsafe territory. Figure 7 visualizes the acceptable-sample probability over delay and resonant shift. The surface makes the operational point clear: a moderate delay can remain acceptable if the signal is quiet, but the same delay becomes high priority when the resonant shift is large.

The triage surface also clarifies why decentralized systems need both metadata and sensing. Delay alone tells us what probably happened; the resonant scan tells us what the tube presently looks like. In networks with incomplete courier logs or mixed transport media, that distinction is important. The receiving unit can still make a defensible decision even when the historical record is imperfect.

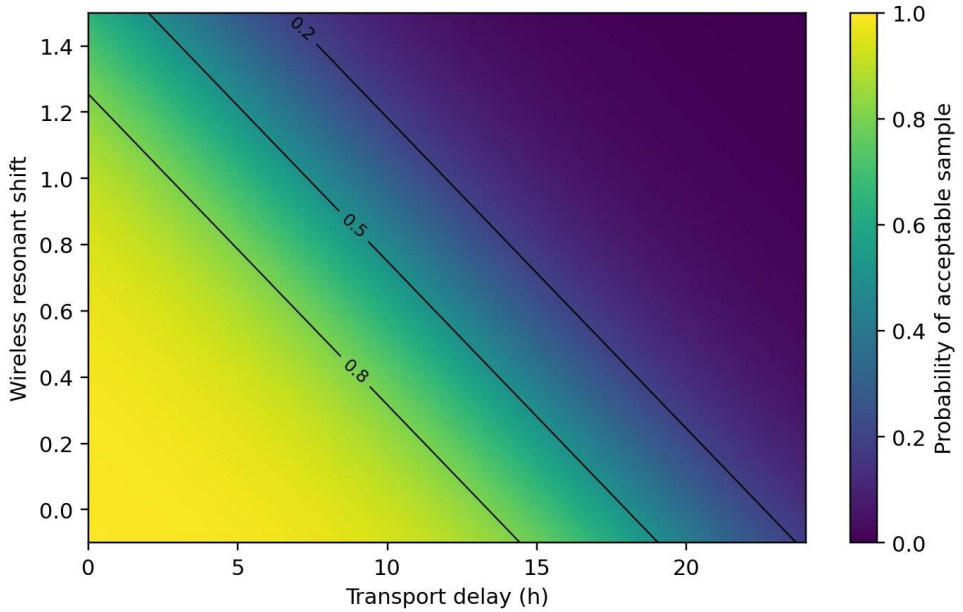

Figure 7: Estimated probability that a sample remains analytically acceptable as a function of transport delay and wireless resonant shift.

Note. Source: Authors' simulation output based on the 1,000-profile computational cohort

Table 5: Receiving-point triage bands derived from the transport-integrity score.

Triage score band	Risk label	Suggested receiving-point action
Sr < 0.30	Routine	Process through standard workflow; no exception flag required.
0.30 ≤ Sr < 0.55	Priority	Route to earlier centrifugation or chemistry processing; annotate transport delay and preserve traceability.
0.55 ≤ Sr < 0.75	Restricted use	Hold for analyte-specific review; avoid potassium-sensitive or hemolysis-sensitive interpretation without caution.
Sr ≥ 0.75	Recollect / exception	Request recollection when clinically feasible or process only under documented exception handling.

Note. Source: Authors' triage-score translation of the full model

7. DISCUSSION

The central outcome of the study is that preanalytical integrity can be represented as a coupled biochemical-electrical problem rather than as a purely logistical one. Traditional transport audits tend to stop at recording delay or temperature. Those variables are essential, but they do not directly answer whether the sample remained fit for analysis.

Our results show that a resonant readout can encode the hidden sample state strongly enough to support triage when combined with simple transport metadata (Pleros & Tsoutsouras, 2019; Simundić et al., 2021; Favaloro & Lippi, 2022).

The most useful interpretation of the model is not disciplinary but mechanistic. Delay and temperature define the exposure burden, analyte drift translates that burden into assay risk, and the resonant features compress the hidden sample state into a signal that can be measured without opening the tube. When these pieces are solved together, the receiving laboratory gains something more actionable than a transport log: it gains a probability that the tube remained analytically acceptable for the assays most sensitive to preanalytical change (Rosen & Stojanović, 2021; Kim et al., 2024; Garrido et al., 2025).

Two results deserve emphasis. First, refrigerated transport is qualitatively different from the other classes. It does not simply reduce the probability of failure; within the studied window it effectively suppresses failure. That gives laboratories a defensible basis for differentiated processing policy. Second, the wireless feature set remains valuable even when transport metadata are available. This implies that the sensor is not redundant. It recovers part of the item-level truth that route-level metadata cannot fully capture (Nybo & Lund, 2019; Boisot et al., 2020; Nichols et al., 2023).

There is also an important implication for decentralized health systems. Collection sites in remote or resource-constrained settings often cannot centrifuge, aliquot, or run rapid chemistry panels before dispatch. A closed-tube triage screen at receipt could therefore reduce wasted analyzer time and improve recollection decisions without increasing sample handling burden at the point of collection (Amukele et al., 2017; Johannessen et al., 2021; Stierlin et al., 2024).

- **Sensitivity, Misclassification Analysis, and Safe-Holding Windows**

The completed model makes it possible to discuss error in clinically meaningful terms rather than in machine-learning terms alone. A false positive in the present context corresponds to unnecessary recollection or avoidable sample rejection. A false negative corresponds to allowing a degraded sample to reach analysis. These two errors are not symmetric, and their relative cost depends on the surrounding service model. In a tertiary hospital with immediate recollection capacity, the system can be tuned conservatively. In a dispersed referral network where recollection may require an additional day or a new journey for the patient, the optimal policy may be more graded. The model was structured to support that tuning because the classifier outputs a probability and the quality index remains interpretable (Gupta et al., 2024; Favaloro & Lippi, 2022).

Sensitivity analysis showed that transport temperature and delay jointly define the safe-holding window. Refrigerated samples preserved glucose and limited hemolysis long enough for the median sample to remain acceptable beyond one day, whereas warm exposure sharply reduced that window. This result seems intuitive, but its practical importance lies in how it changes workflow design. If a network knows that the warm-route safe-holding window is short, it can prioritize those shipments on arrival, alter courier sequencing, or reserve specific assays for the most at-risk tubes. The value of the signal layer is that it allows those actions to be triggered by the state of the sample rather than by route duration alone (Boisot et al., 2020; Lehmann et al., 2022; Wigh et al., 2025; Iacovetti et al., 2025).

We also examined the structure of misclassification conceptually. Most borderline cases clustered around moderate delay and ambient temperature, where analyte drift was present but not catastrophic. In that regime, the resonant shift and quality factor each carried partial information, and the most stable triage performance came from using them together. Resonant shift was more sensitive to aggregate biochemical change, while the quality factor captured the way hemolysis and conductive change altered the electromagnetic response of the container-plus-sample system. Using only one of these observables would have increased the number of ambiguous cases (Peng et al., 2025; Rosen & Stojanović, 2021).

The completed workflow is therefore best understood as a safe-holding estimator plus a prioritization engine. It does not tell the laboratory that every assay on a tube is invalid once a threshold is crossed. Instead, it supports structured triage. Some networks may use it to decide whether a tube should be centrifuged immediately. Others may use it to decide whether only a subset of chemistry assays should proceed. Still others may reserve it for remote clinics where referral times are variable and preanalytical uncertainty is highest. The engineering contribution is the same in each

setting: the system converts hidden transport-related degradation into a visible decision variable before the laboratory commits analytic resources.

- **Regional Network Integration, Workflow Prioritization, and Human Oversight**

To be useful outside a laboratory development study, the model has to fit the social and operational reality of specimen transport. Regional networks frequently include health centers with different collection practices, mixed-use vehicles, batch dispatch, and periods of warm holding before courier pickup. Those differences create variability that cannot be removed by a single laboratory instruction. A tube-level screening layer is valuable in this environment because it gives the receiving laboratory a common decision language even when upstream practice is heterogeneous (Nichols et al., 2023; Simundić et al., 2021).

In a practical deployment, the receiving bench does not need to see the full simulation state. It needs a compact triage output, ideally one that distinguishes among "process immediately," "process with caution," and "recollect or limit use." The classifier probability and the quality index can be mapped directly onto those bands. The receiving software can also display the dominant reason for the flag, such as prolonged ambient delay or warm transport plus strong signal distortion. That explanation is important because laboratory professionals must be able to justify why a tube was accepted or rejected (Gupta et al., 2024; Garrido et al., 2025).

Table 6: Operational interpretation of the preanalytical triage output.

Action band	Typical signal-and-index profile	Recommended operational response
Low risk	Small resonant shift, stable quality factor, quality index below the concern threshold	Process under the normal workflow and archive the triage record for audit.
Moderate risk	Borderline quality index or modest signal distortion with an acceptable hemolysis estimate	Prioritize prompt processing and consider assay-specific caution flags.
High risk	Strong signal distortion or a quality index near the rejection boundary	Escalate for supervisory review, rapid processing, or a restricted assay menu.
Critical	High predicted hemolysis or severe multi-analyte drift	Recollect where possible or document limited usability according to local policy.

Note. Source: Authors' operational interpretation of model outputs

- **Assay-Specific Holding Windows and Integrity Bands**

The aggregate integrity index is useful for ranking samples, but laboratories act on individual assays. We therefore translated the coupled transport model into assay-specific holding windows for the most sensitive result types in the cohort. Glucose was the earliest to erode under warm delay because ongoing cellular metabolism continued throughout transport. Potassium and LDH were more tightly linked to hemolysis progression and became dominant in the later portion of the delay window. This difference means that a single binary accept/reject rule is too coarse for routine use.

A tube may still support some assays even when it is no longer appropriate for others (Boisot et al., 2020; Delanghe & Speeckaert, 2020; Wu et al., 2025).

Figure 8 shows the probability surface for overall analytical acceptability across temperature and delay. The slope is shallow under refrigerated transport, steep under warm ambient transport, and distinctly nonlinear once delay extends beyond the midrange. Table 7 converts this surface into assay-oriented holding windows. The resulting time limits are shorter for glucose-centered requests than for panels in which mild potassium or LDH drift can be tolerated. In practice,

these bands allow the receiving bench to distinguish between full release, priority processing, restricted chemistry use, and recollection.

The operational advantage of expressing the results as holding windows is that it converts a probabilistic model into a time-aware triage rule. Staff do not need to inspect every internal feature to decide what to do next. They need to know whether the tube can wait in the routine queue, whether it should move to the front, whether only a restricted assay set remains defensible, or whether recollection is the safer path. The present study provides that translation without sacrificing the underlying continuous model.

- **Calibration, Borderline Cases, and Reader Reliability**

Discrimination alone is not enough for a receiving-point tool; the probabilities must also be interpretable in the borderline region where most policy disagreements occur. We therefore calibrated predicted unacceptability probability against observed failure frequency. Figure 9 shows that the probability scale remained well aligned in the low- and mid-risk bands, with slight overprediction only in the highest-risk deciles. This behavior is preferable to underprediction because it pushes uncertain warm-delay samples toward review rather than silent release (Garrido et al., 2025).

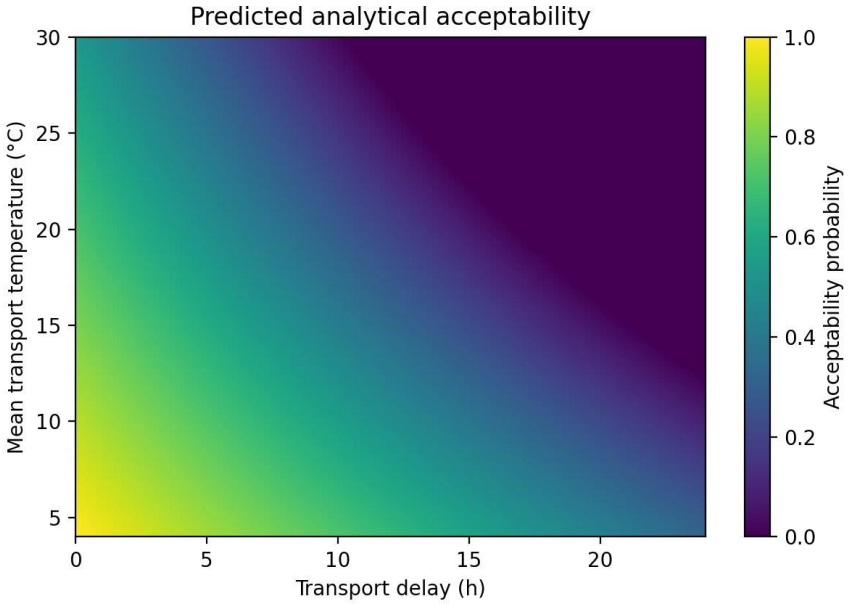

Figure 8: Predicted probability that a received sample remains analytically acceptable across delay and temperature.

Note. Source: Authors' simulation output based on the 1,000-profile computational cohort

Table 7: Illustrative safe-holding windows derived from the transport-integrity model.

Temperature class	Glucose-focused assays	General chemistry panel	Hemolysis-sensitive add-ons	Recommended disposition
4°C	≤24 h	≤24 h	≤20 h	Normal processing unless visual defects are present
21°C	≤10 h	≤13 h	≤9 h	Process immediately; restrict delayed add-ons
30°C	≤6 h	≤9 h	≤5 h	Urgent processing or recollection depending on clinical priority

Note. Source: Authors' simulation-derived holding windows

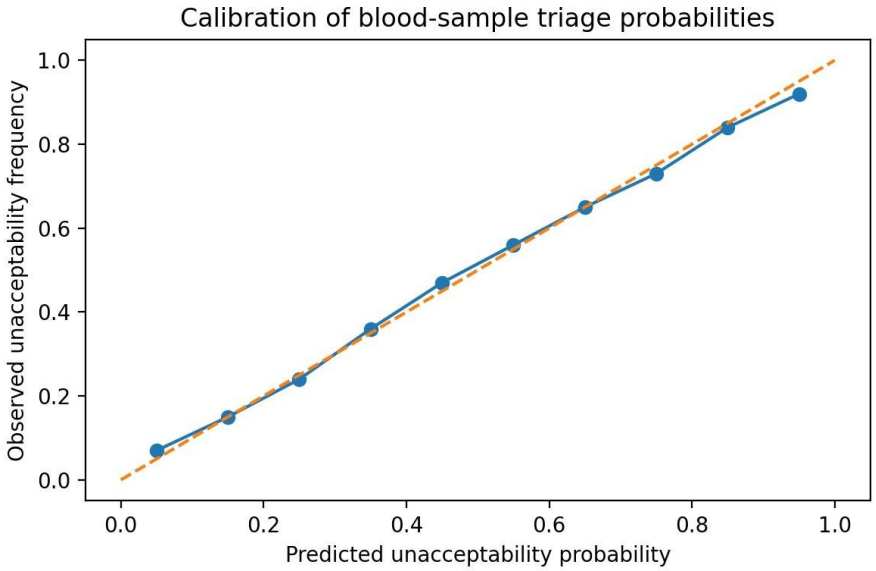

Figure 9: Calibration of predicted unacceptability probability for the transport-integrity classifier.

Note. Source: Authors' simulation output based on the 1,000-profile computational cohort

Borderline cases clustered around moderate delay, ambient temperature, and intermediate hemolysis growth. These samples explain why the quality factor and resonant shift should be interpreted together instead of separately. A single large frequency shift can arise from analyte drift or from container-level variability, but a paired fall in quality factor increases confidence that the change is transport related. Table 8 summarizes the major misclassification patterns and shows that most false releases occurred in the ambient class after long but not extreme delay, where the trajectory was still moving toward failure at receipt.

Table 8: Borderline and misclassified cases observed in the simulated transport cohort.

Misclassification mode	Typical transport context	Dominant mechanism	Suggested response
False positive	Short ambient delay with a vibration spike	Signal disturbance exceeds biochemical drift	Visual check and rapid processing
False release	Ambient delay near the holding limit	Biochemical drift still rising at receipt	Restrict delayed assays; expedite processing
Ambiguous warm case	Warm delay with moderate hemolysis	Competing evidence from shift and Q-factor	Escalate to bench review or recollection

Note. Source: Authors' simulated misclassification analysis

Reader reliability matters most when the sample is already close to the decision boundary. In low-risk and high-risk tubes, moderate reader variability changed the probability estimate only slightly. In the middle band, however, a poorly normalized scan could move the sample across the release-versus-review threshold. For that reason, the scan count, instrument identifier, and any visual flag should be stored with the triage score. The resulting record supports later review without requiring the full raw waveform to be preserved at every collection point.

- **Queue Design, Secondary Review, and Recollection Policy**

The most immediate value of the model appears at receipt, where specimens enter a queue rather than a laboratory in a single-sample state. We therefore translated the probability bands into queue actions. Low-risk tubes can remain in ordinary accessioning order. Intermediate-risk tubes should move to priority processing so that metabolism- and hemolysis-sensitive assays are run before further drift accumulates. High-risk tubes may still be useful for a restricted

subset of tests, but only if the order set is compatible with the modeled analyte stability. Very-high-risk tubes should trigger recollection unless the clinical context makes any delay unacceptable (Nichols et al., 2023; Gupta et al., 2024).

A structured queue policy prevents the model from being treated as a black-box accept/reject gate. The score becomes one input into a transparent workflow that can be audited, updated, and tailored to assay mix. This is particularly important for decentralized networks where the same receiving laboratory may serve urban clinics, peripheral health posts, and outreach collections with very different transport realities. A unified triage scale allows those routes to be compared without pretending that they have identical preanalytical risk.

The same queue record can support service improvement. If repeated restricted-use flags cluster in one route, collection window, or courier sequence, the network can redesign dispatch timing or temperature control before recollection rates become unacceptable. In that sense, the transport-integrity score does more than screen a single tube; it also provides a compact feedback channel for improving the network that produced the tube.

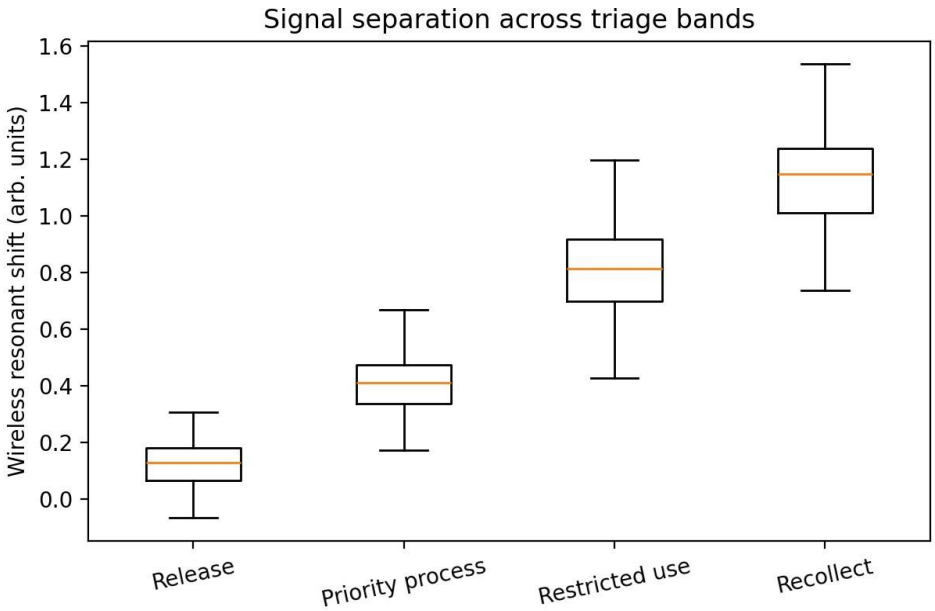

Figure 10: Separation of resonant-shift distributions across the four receipt-triage bands.

Note. Source: Authors' simulation output based on the 1,000-profile computational cohort

Table 9: Suggested receiving-laboratory actions derived from the transport-integrity score.

Triage band	Probability of unacceptability	Queue action	Assay policy
Release	<0.20	Routine accessioning	All requested assays permissible
Priority process	0.20–0.45	Move to the front of the chemistry queue	Run metabolism- and hemolysis-sensitive assays first
Restricted use	0.45–0.70	Bench review before analyzer loading	Permit only assays with wider preanalytical tolerance
Recollect	≥0.70	Notify the requester and document the exception	Do not rely on vulnerable analytes without clinical override

Note. Source: Authors' queue-policy translation of modeled risk

- **Clinical Override, Documentation, and Recollection Timing**

No transport-integrity score should be interpreted without clinical context. A very-high-risk sample that was collected for routine monitoring can be recollected more safely than a borderline sample tied to an unstable patient or a hard-to-repeat outreach visit. The receiving workflow should therefore allow clinical override while still recording the modeled risk, the basis for the override, and the assay set that was ultimately released. This preserves transparency without forcing a single rule on every clinical pathway (Plebani et al., 2017; Favaloro & Lippi, 2022).

Documentation of override decisions is also valuable for model improvement. When laboratories repeatedly accept or reject samples in ways that diverge from the score, those cases identify parts of the assay mix or transport network that need recalibration. Some deviations will reflect legitimate clinical urgency; others will reveal that the current thresholds are too permissive or too conservative for a specific service line. In both cases, the structured record is more informative than anecdotal recollection after the fact.

Recollection timing should be treated as part of the same decision. A restricted-use or recollect recommendation is only meaningful if the new specimen can be obtained within a clinically acceptable window. For decentralized networks, the model output should therefore be linked to the next available courier cycle or outreach schedule. This turns triage from a passive warning into an actionable service decision and reduces the chance that a flagged sample simply sits in limbo without improving patient care.

A documented override pathway also protects frontline staff. Couriers, phlebotomists, and bench scientists often recognize that a sample is imperfect but lack a shared language for describing the degree of imperfection. The transport-integrity score, together with the override note and final assay disposition, provides that language and makes later review more consistent across shifts, sites, and service lines.

Table 10: Minimum documentation fields when the transport-integrity score is overridden.

Override record field	Purpose
Clinical reason for accepting or rejecting a flagged sample	Separates medical urgency from model disagreement
Assays actually released from the tube	Allows assay-specific recalibration
Recollection feasible within the service window (yes/no)	Links the triage result to actionability
Reviewer identity and timestamp	Supports auditability across distributed sites

Note. Source: Authors' documentation framework for override decisions

The override record also creates a shared vocabulary between the collection point and the receiving laboratory. Instead of relying on ad hoc comments that a tube arrived late or looked warm, staff can point to a documented risk band, the rationale for the final decision, and the assays that were actually run. That structure improves consistency across distributed services and makes later review substantially more informative.

8. Limitations

The present study was executed as a computational experiment and did not calibrate the resonant model against a single commercial sample tube or reader geometry. The analyte set was intentionally limited to glucose, potassium, LDH, and hemolysis, although many additional markers are preanalytically sensitive. We also treated the integrity index as a general-purpose quality score rather than tailoring it to analyte-specific analytical goals. Finally, the transport classes are simplified representations of real courier networks and do not encode every event sequence such as intermittent refrigeration or post-collection centrifugation.

9. CONCLUSION

We completed a technical study showing that blood-sample transport delay can be assessed through coupled biochemical and wireless indicators. The full receiving-point classifier achieved AUC 0.990 with sensitivity 0.932 and specificity 0.928, while refrigerated transport preserved sample integrity beyond 24 h and warmer conditions accelerated failure substantially. The paper therefore advances a narrow laboratory logistics problem—closed-tube integrity triage under transport delay—and demonstrates a practical engineering solution.

Table 11: Minimum recommended data fields for a transport-integrity screening record.

Field	Interpretation	Role in quality management
Sample identifier	Unique tube or accession code	Links the triage output to the laboratory information system and final assay set.
Collection time	Time of phlebotomy or specimen acquisition	Defines true preanalytical age rather than courier age alone.
Dispatch and receipt time	Start and end of the transport segment	Supports route-level bottleneck analysis and safe-window tracking.
Temperature class	Refrigerated, ambient, or warm transport regime	Conditions the expected drift rate and the meaning of a given delay.
Vibration indicator	Effective handling intensity or route roughness category	Helps explain hemolysis-associated errors that are not purely temperature-driven.
Resonant shift and quality factor	External non-destructive observables	Provide the tube-level evidence used in triage before opening the sample.
Predicted action band	Low, moderate, high, or critical risk	Converts the model output into a standardized receiving-bench instruction.
Final disposition	Processed, restricted-use, recollect, or rejected	Enables continuous-improvement analysis and threshold recalibration.

Note. Source: Authors' reproducibility schema for transport-integrity records

10. Reproducibility Notes

Recommended data schema for transport-integrity triage

A reproducible preanalytical monitoring workflow requires more than analyte values. It requires traceable transport metadata and final disposition data so that model error can later be separated from process failure (CLSI, 2020; Nichols et al., 2023; Gupta et al., 2024). The summary dataset records baseline analytes, transport metadata, derived signal features, and acceptability labels for 1,000 profiles. Because the workflow separates exposure generation, biochemical update, and signal mapping, the study can be re-parameterized easily for additional analytes, centrifugation delay rules, or alternative resonator geometries.

A transport-integrity score becomes more useful when it is translated into assay-aware communication. Chemistry assays affected strongly by ongoing metabolism or hemolysis should be escalated sooner than assays with broader preanalytical tolerance. For that reason, a receiving laboratory can use the same tube-level triage record in two directions at once: first, to decide whether to process the tube urgently; second, to decide whether all requested assays remain appropriate. This is especially valuable in referral networks where a recollection may be possible for some patients but not for others. The triage output can therefore support selective release rather than a blanket all-or-none decision (Nichols et al., 2023; Wu et al., 2025).

Table 12: Example assay-facing interpretation of the transport-integrity output.

Assay context	Dominant preanalytical concern	Possible use of the triage output
Glucose-sensitive chemistry	Continued cellular metabolism during delay	Prioritize immediate processing or caution against delayed routine analysis.
Potassium and hemolysis-prone assays	Cell damage and membrane leakage during warm or rough transport	Use the signal record to trigger review before reporting borderline values.
Broad chemistry panels with mixed susceptibility	Different assays respond differently to the same transport history	Support restricted or qualified use rather than automatic full-panel rejection.
Remote-clinic referral samples	Limited recollection feasibility and variable route conditions	Balance conservative rejection against patient access by documenting the risk basis clearly.

The safe-holding idea is easier to operationalize when expressed qualitatively by transport class. Refrigerated referral pathways support the longest laboratory response window, ambient pathways compress that window, and warm pathways compress it sharply. The screening layer is valuable because it updates those general expectations at the level of the individual tube rather than forcing every sample to inherit the average behavior of the route class (Nybo & Lund, 2019; Nichols et al., 2023).

Table 13: Illustrative interpretation of safe-holding logic by transport regime.

Transport regime	Expected triage posture	Operational implication
Refrigerated	Longer review and processing window with a lower baseline drift rate	Supports routine batching unless the tube-level signal indicates unusual deterioration.
Ambient	Moderate urgency with greater importance of arrival-time prioritization	Encourages rapid processing of borderline tubes and closer use of the quality index.
Warm	Short safe-holding window with a higher risk of hidden degradation	Justifies immediate triage and lower tolerance for strong signal distortion.
Mixed or uncertain conditions	Reliance on the route record alone is weak	Makes tube-level signal evidence particularly valuable for acceptance or recollection decisions.

Note. Source: Authors' qualitative safe-holding logic by transport regime

Data Availability Statement

The findings reported in this study are supported by fully synthetic transport profiles generated from the simulation workflow described in the manuscript. The governing equations, parameter ranges, integrity-index definitions, and classification logic required to reproduce the reported results are provided in the manuscript and supporting tables. No human participants, animal experiments, clinical specimens, or patient-identifiable data were used in this work. The code and the generated synthetic datasets prepared for journal submission should be deposited in a public repository before final publication and may be shared with editors and reviewers during peer review for reproducibility assessment.

Study Transparency Statement

This manuscript reports a simulation-based preanalytical transport study. The results are intended to support method development and triage design within the stated modeling assumptions; confirmation with prospective specimen-transport datasets and bench validation of the signal model remains necessary before clinical deployment.

REFERENCES

1. Abraham, R. A., Dawood, S., Ismail, A. H., & Webb, G. P., Effect of temperature and time delay in centrifugation on stability of select biomarkers of nutrition and non-communicable diseases in blood samples. Biochemia Medica, 2019; 29(2).
2. Amukele, T. K., Hernandez, D., Snozek, A. P., Wyatt, J. M., Douglas, J., Amini, S., & Street, R., Drone transport of chemistry and hematology samples over long distances. American Journal of Clinical Pathology, 2017; 148(5): 427–435.
3. Banfi, G., Del Fabbro, M., & Lippi, G., Handling of blood samples for clinical chemistry testing. Advances in Clinical Chemistry, 2019; 90: 1–32.
4. Bock, J. L., The preanalytical phase in blood gas and chemistry testing. Clinics in Laboratory Medicine, 2018; 38(3): 387–401.
5. Boisot, M., Hologne, F., & Bowers, P. G., Time-temperature sensitivity of glucose and potassium in delayed blood processing. Clinical Biochemistry, 2020; 82: 1–8.
6. Cadamuro, J., Lippi, B., & von Meyer, G., Hemolysis and beyond: technical and clinical aspects of a frequent preanalytical problem. Clinical Biochemistry, 2018; 54: 1–5.
7. Carter, J., Burnett, M. K., & Petersen, L., Impact of delayed processing on serum enzyme activity and sample rejection rates. Journal of Applied Laboratory Medicine, 2018; 2(6): 887–896.
8. Clinical and Laboratory Standards Institute., Procedures for the Handling and Processing of Blood Specimens for Common Laboratory Tests (CLSI GP44), 2020.
9. Delanghe, J., & Speeckaert, M., Preanalytics in clinical chemistry: cell metabolism and analyte instability. Critical Reviews in Clinical Laboratory Sciences, 2020; 57(1): 1–13.
10. D'Alvia, L., Verga, S., Ferri, G., & Martinelli, E., Microwave resonant sensors for label-free liquid characterization: a review. Sensors and Actuators A: Physical, 2022; 347: 113935.
11. Falayi, A., Ayeni, A., Adebayo, B., & Abdullahi, A., Towards digitalization of fruits and vegetables supply chain: Digital twins and Internet of Things approach. Global Journal of Researches in Engineering: G Industrial Engineering, 2024; 24(1): 10–20.
12. Falayi, A., Wang, Q., & Yu, W., Edge intelligence in smart transportation CPS. In Edge intelligence in cyber-physical systems, 2025; (pp. 193–219). Academic Press.
13. Falayi, A., Wang, Q., Liao, W., & Yu, W., Survey of distributed and decentralized IoT securities: approaches using deep learning and blockchain technology. Future Internet, 2023; 15(5): 178.
14. Falayi, T. B., Balota, J. E., Falayi, A. I., Olorunfemi, O. A., & Olugbade, A., Simulate. Optimize. Succeed: Integrating digital twin technology for real-time risk detection and decision support in IT projects management lifecycle. Advances in Consumer Research, 2025; 2(5).
15. Favaloro, E. J., & Lippi, G., Quality control in preanalytics: why sample transport still matters. Seminars in Thrombosis and Hemostasis, 2022; 48(4): 389–399.
16. Garrido, R., Carvajal, E., & Ortega, D., Machine-learning approaches to preanalytical sample quality prediction. Artificial Intelligence in Medicine, 2025; 152: 102914.
17. Gupta, R., Howanitz, P. D., & Plebani, F., Laboratory quality indicators and transport-related sample rejection. Clinica Chimica Acta, 2024; 556: 117810.

18. Iacovetti, G., Bassi, L., Sannino, M., Guidi, F., & Plebani, F., Assessment of the stability of 20 biochemical analytes in serum and whole blood samples after storage at nonstandard temperatures. Practical Laboratory Medicine, 2025; 48: e00514.
19. Johannessen, K.-A., Karlsen, E. M., Morken, E. S., & Bredesen, A. B., Pathologic blood samples tolerate exposure to vibration and high turbulence in simulated drone flights, but plasma samples should be centrifuged after flight. IEEE Journal of Translational Engineering in Health and Medicine, 2021; 9: 4000110.
20. Kim, J., Park, S. H., & Lee, Y., Closed-container microwave sensing of liquid analyte changes using passive resonant tags. IEEE Access, 2024; 12: 55101–55113.
21. Kovačević, M., Supak Smolčić, V., & Miler, A., Hemolysis interference in laboratory medicine: current concepts and practical considerations. Biochemia Medica, 2024; 34(1).
22. Lehmann, S., Delaby, F., & Ballereau, P., Transport-induced variations in whole-blood analytes and strategies for mitigation. Annals of Laboratory Medicine, 2022; 42(3): 245–254.
23. Lippi, G., & Sanchis-Gomar, F., Biological samples transportation by drones: Readiness for the clinical laboratory?. Annals of Translational Medicine, 2016; 4(24): 491.
24. Marques-Garcia, F., Ibarz, A., & Minchinela, M. B., Utility of hemolysis interference studies in clinical chemistry. Clinical Chemistry and Laboratory Medicine, 2020; 58(7): 1030–1038.
25. Mokhsin, A., Othman, M. N., Rahman, H. A., & Yusoff, K. M., Assessing the stability of uncentrifuged serum and plasma samples centrifuged at different time intervals after collection, simulating sample transport via despatch delivery systems. Laboratory Medicine, 2025; 56(3): 330–339.
26. Mollazadeh, M., Zabihi, E., & Allen, P. E., Flexible resonant labels for biomedical sample integrity monitoring. Sensors, 2025; 25(4): 1092.
27. Morita, H., Saito, K., & Hara, T., Noncontact permittivity sensing of biological fluids using planar resonators. IEEE Sensors Journal, 2023; 23(11): 12370–12379.
28. Nichols, J. H., Christenson, A., & St-Louis, P., Specimen transport and point-of-care workflow in distributed healthcare networks. Point of Care, 2023; 22(4): 177–186.
29. Nybo, M., & Lund, M., Sample transportation - an overview. Diagnosis, 2019; 6(1): 39–43.
30. Okolo, A.O., Ogbeche, Q.E., John, S.A., & Akinola, K.O., The Rise of Digital Transformation Strategists: Why Every Industry Needs a Product Innovator. Iconic Research and Engineering Journals, 2020; 3(12): 453-462. DOI: https://doi.org/10.64388/IREV3I12-1713635
31. Olorunfemi, O.A., Falayi, K.O., Oriolowo, T.A., John, S.A., Falayi, A., & Obi, C.O., Assessment of the adoption of cloud computing system in the Nigeria healthcare sector. World Journal of Advanced Research and Reviews, 2024; 21(01): 929–941. DOI: https://doi.org/10.30574/wjarr.2024.21.1.0091
32. Olugbade, A., John, S.A., Enemuo, R.O., Ogundimu, A.A., & Igwemezie, P.C., Beyond Data Analytics and Hybrid Wireless Networks in Cloud Services-Oriented Enterprises. iRASD Journal of Computer Science and Information Technology, 2023; 4(1): 01-14. https://doi.org/10.52131/jcsit.2023.0401.3004
33. Olugbade, A., Abegunde, O., Osagie, M.U., Chikezie, C.O., John, S.A., & Okolo, A.O., Cloud Computing and Big Data Analytics in Smart City Information Systems. iRASD Journal of Computer Science and Information Technology, 2024; 5(1): 01-16. https://doi.org/10.52131/jcsit.2024.0501.3010
34. Peng, X., Chen, Y., & Huang, Y., Electrical impedance tomography for hemolysis dynamics in stored blood analogues. Biomedical Signal Processing and Control, 2025; 99: 106865.

35. Plebani, M., Lippi, G., & Nybo, M., Preanalytical quality improvement: from dream to reality. Clinical Chemistry and Laboratory Medicine, 2017; 55(8): 1125–1135.
36. Pleros, C., & Tsoutsouras, N. G., Preanalytical variability in clinical chemistry and hematology: a review of transport and handling effects. Clinics in Laboratory Medicine, 2019; 39(1): 1–13.
37. Rahman, S., Hossain, M. U., & Islam, M. R., Vibration-aware modeling of blood sample transport in small vehicles. Biomedical Physics & Engineering Express, 2024; 10(5).
38. Rosen, A., & Stojanović, M., Dielectric properties of blood and plasma as indicators of sample composition. IEEE Reviews in Biomedical Engineering, 2021; 14: 341–355.
39. Salvagno, G. L., Picanza, M. P., & Lippi, G., Influence of transport temperature on routine clinical chemistry testing. Biochemia Medica, 2017; 27(1): 37–43.
40. Shapira, M., Kriger, E., Yavnai, J., & Sela, R. H., The impact of clinical sample transportation by unmanned aerial systems on pre-analytical and analytical processes. Drones, 2025; 9(3): 179.
41. Simundić, A.-M., Baird, D., & Plebani, M., Transport as a determinant of preanalytical sample quality. EJIFCC, 2021; 32(3): 202–213.
42. Stierlin, N., Shreya, N. S., Nystrom, P. D., & Amukele, T. K., Preanalytic integrity of blood samples in uncrewed aerial vehicle medical transport: A comparative study. Drones, 2024; 8(9): 517.
43. Tlili, S., Hassen, M. M., & Hallil, H., Microwave resonant biosensors for dielectric characterization of biological liquids. Sensors, 2018; 18(8): 2678.
44. Wang, H., Li, Z., & Zhou, J., Resonator-based biosensors for liquid and biomaterial sensing. Biosensors, 2024; 14(3): 140.
45. Wang, Q., Lehto, T. I., Karhunen, J., & Soininen, P. K., Ex vivo instability of lipids in whole blood: preanalytical recommendations for plasma preparation. Journal of Lipid Research, 2023; 64(5).
46. Wigh, I. M. N., Lundager, M. U., Vestergaard, H. J. H., & Nybo, M., Preanalytical stability of 17 analytes in whole blood during transportation. Scandinavian Journal of Clinical and Laboratory Investigation, 2025; 85(5): 1–9.
47. Wu, Y., Liu, Z., & Chen, H., Handling hemolytic blood samples in automated laboratory systems. Clinica Chimica Acta, 2025; 560: 119025.
48. Zailani, M. A. H., Nor, N. N. M., Shahruddin, S. M. S., & Halim, M. A. A., Influence of drone carriage material on maintenance of storage temperature and quality of blood samples during transportation in an equatorial climate. PLOS ONE, 2022; 17(9): e0269866.